

Aggregation enhanced emission (AEE) in organic salt: A structure-property correlation based on single crystal studies

UTTAM KUMAR DAS and PARTHASARATHI DASTIDAR*

Department of Organic Chemistry, Indian Association for the Cultivation of Science, 2A & 2B Raja S C
Mullick Road, Jadavpur, Kolkata 700 032, West Bengal, India
e-mail: ocpd@iacs.res.in

MS received 19 May 2014; revised 21 August 2014; accepted 1 September 2014

Abstract. Salt formation has been shown as a simple strategy to induce aggregated induced emission or aggregated enhanced emission in primary ammonium salts derived from 9-anthracene carboxylic acid, 1-pyrene carboxylic acid, 3-coumarin carboxylic acid and histamine. All the salts displayed enhanced fluorescence in their solid state compared to that in their solution state. Single crystal structure of the salt of 9-anthracene carboxylic acid i.e., His-anthracene revealed that restricted intramolecular rotation of the fluorophoric moiety (anthracene) was responsible for such radiative pathway leading to enhanced emission.

Keywords. AIE; AEE; single crystal; salt, crystal engineering.

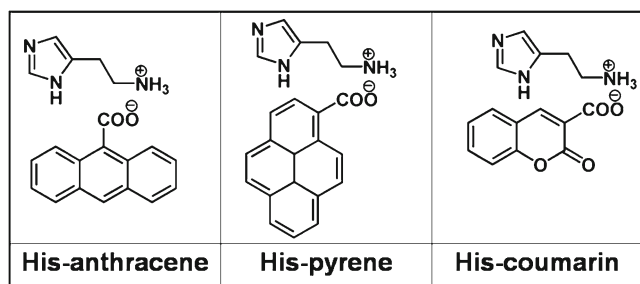
1. Introduction

Light emitting properties like luminescence or fluorescence are well-known and well-studied phenomenon in the molecular world.¹ Usually, photophysical studies are carried out in a highly dilute solution so that the molecule under study can almost be considered as 'isolated'.² However, when the molecule is not isolated and kind of forced to aggregate either due to solvophobic effect or crystallization, emission behaviour of the molecule is immensely affected and in most of the cases, luminescence is greatly reduced or quenched – a phenomenon widely known as 'aggregation-caused quenching' or ACQ. The reason for such quenching is attributed to the mechanical restriction due to aggregation. ACQ phenomenon is most common to the fluorophores containing aromatic moieties.³ It has been proposed that ACQ occurs because of the possible $\pi - \pi$ interactions involving the large π -surface usually present in fluorescent molecules leading to the formation of excimers or exciplexes. It is understandable that ACQ is an impediment in real-life applications of luminescence materials. For example, luminescent molecules are often used as sensors in aqueous media wherein the highly hydrophobic luminescent moieties are expected to aggregate, leading to ACQ thereby reducing the sensitivity of the sensors.^{4–8}

In 2001, Tang *et al.* reported a counter-intuitive phenomenon which they termed as 'aggregation-induced

emission' (AIE). They observed that a series of phenyl substituted siloles were non-emissive in dilute solution whereas they were highly fluorescent in the solid state.^{9,10} Such counter-intuitive phenomenon was explained by invoking the concept of restricted intramolecular rotation (RIR) in aggregated state. It is well known that molecular motion consumes energy. In dilute solution, the peripheral phenyl rings in these silole derivatives can freely rotate along the single bond between the phenyl ring and silole moiety thereby allowing a relaxation channel for the excited molecules. On the other hand, when RIR comes into play in aggregated state, the excited molecules are forced to take a radiative pathway causing emission or AIE. Scientists around the world immediately realized soon after this serendipitous discovery that AIE has significant technological implications. Instead of passively working against aggregation in order to avoid ACQ, one can deliberately design molecule that would reinforce RIR in aggregated state thereby causing AIE. In fact, a plethora of reports vis-à-vis designing molecules with AIE property poured in.^{11–15} Typically in AIE active molecule, the rotor (e.g., phenyl ring) rotates freely in solution against the stator (e.g., silole moiety) thereby making it non-emissive, whereas such free rotations are restricted in aggregated state causing AIE. During attempts to design AIE materials, luminescent moieties are installed on a polymeric chain causing a certain degree of RIR thereby enabling emission in the solution state.^{16,17} Such RIR is reinforced in aggregated state causing enhanced emission and such

*For correspondence



Scheme 1. The PAM salts under study.

molecules are aggregation-enhanced emission (AEE) active.

Herein, we demonstrated salt formation as a simple strategy to impose AEE activity. Thus, a new series of simple organic salt was synthesized from three fluorophoric carboxylic acids namely anthracene-, pyrene- and coumarin carboxylic acid and histamine (scheme 1). It was observed that photoluminescence of the salts were enhanced manifolds compared to that of the solution state demonstrating AEE activity in these salts. With the help of single crystal structure of His-anthracene, a structure-property correlation was attempted.

2. Experimental

2.1 Materials and physical measurements

All the starting materials were commercially available which were used without further purification. Solvents were of L.R. grade and used without further distillation. Both ^1H and ^{13}C NMR spectra were collected using 500 MHz spectrometer (Bruker Ultrashield Plus-500) and a 400 MHz spectrometer (Bruker AscendTM-400). FT-IR spectra were obtained using an FTIR instrument (FTIR-8300, Shimadzu). The elemental compositions of all the purified compounds were confirmed by elemental analysis using Perkin-Elmer Precisely, Series-II, CHNO/S Analyser-2400.

2.2 Syntheses

Except 3-cumarine carboxylic acid (855 mg, 4.5 mmol), the other two acids were not soluble in MeOH. The salts were thus prepared by adding solid acids (1107 mg, 4.5 mmol of pyrene-1-carboxylic acid and 1000 mg, 4.5 mmol of 9-anthranic acid) into methanolic solution of histamine (500 mg, 4.5 mmol). The resultant mixture became homogeneous solutions which upon

evaporation in rotary evaporator yield the corresponding salts. All the salts were characterized by NMR (^1H and ^{13}C), FT-IR and elemental analysis. Salt formation was confirmed by the absence of the bands ($>\text{C}=\text{O}_{\text{COOH}}$ at $1650\text{--}1700\text{ cm}^{-1}$) for the parent acids and the presence of sharp bands in the range of $1524\text{--}1645\text{ cm}^{-1}$ ($>\text{C}=\text{O}_{\text{COO}^-}$).

2.3 His-pyrene

Elemental analysis calcd for $\text{C}_{22}\text{H}_{21}\text{N}_3\text{O}_2\cdot\text{H}_2\text{O}$ (%): C 70.38, H 5.64, N 11.19; found: C 70.43, H 5.48, N 11.19; ^1H NMR (500MHz, $\text{DMSO-}d_6$): δ (ppm) = 9.30 (d, $J = 9.5$ Hz, 1H); 8.41 (d, $J = 8$ Hz, 1H); 8.25 (t, $J = 7.5$ Hz, 2H); 8.21 (d, $J = 8$ Hz, 1H); 8.1 (m, $J = 7.5$ Hz, 3H), 8.05 (t, $J = 7.5$ Hz, 1H), 7.58 (s, 1H), 6.89 (s, 1H), 3.08 (t, $J = 7.5$, 2H), 2.86 (t, $J = 7.5$, 2H); ^{13}C NMR (400MHz, $\text{DMSO-}d_6$): δ (ppm) = 171.88, 135.69, 134.94, 130.78, 130.68, 128.19, 127.32, 127.20, 127.15, 126.88, 126.60, 125.93, 124.93, 124.76, 124.18, 124.02, 124.00, 48.54 and 25.77; FT-IR (KBr pellet): 3439, 3417, 3047, 2885, 1645 ($>\text{C}=\text{O}_{\text{COO}^-}$), 1585, 1568, 1501, 1383, 1356, 1313, 1218, 1178, 1150, 1086, 1030, 968, 945, 879, 845, 789, 763, 716, 619, 457 and 413 cm^{-1} .

2.4 His-anthracene

Elemental analysis calcd for $\text{C}_{20}\text{H}_{19}\text{N}_3\text{O}_2$ (%): C 72.05, H 5.74, N 12.60; found: C 70.79, H 5.70, N 12.17; ^1H NMR (500MHz, $\text{DMSO-}d_6$): δ (ppm) = 8.36 (s, 1H), 8.15 (d, $J = 8.5$ Hz, 2H); 8.01 (d, $J = 8.5$ Hz, 2H); 7.51 (s, 1H); 7.44 (m, 4H); 6.84 (s, 1H); 3.04 (t, $J = 7.5$ Hz, 2H); 2.82 (t, $J = 7.5$ Hz, 2H); ^{13}C NMR (400MHz, $\text{DMSO-}d_6$): $\delta = 172.06$, 140.44, 134.94, 131.02, 127.82, 127.25, 125.92, 124.99, 124.51, 123.58, 48.05 and 25.30; FT-IR (KBr pellet): 3107, 3053, 2960, 2856, 2787, 2721, 2669, 2610, 1639 ($>\text{C}=\text{O}_{\text{COO}^-}$), 1582, 1526, 1503, 1492, 1440, 1427, 1389, 1277, 1220, 1180, 1103, 1025, 1010, 997, 941, 885, 862, 845, 827, 798, 784, 739, 656, 600, 576 and 444 cm^{-1} .

2.5 His-coumarin

Elemental analysis calcd for $\text{C}_{21}\text{H}_{20}\text{N}_4\text{O}_5$ (%): C 59.79, H 5.02, N 13.95; found: C 58.39, H 5.33, N 13.26; ^1H NMR (400MHz, $\text{DMSO-}d_6$): δ (ppm) = 8.47 (s, 1H); 8.13 (s, 1H); 8.06 (d, $J = 9.2$ Hz, 1H); 7.72 (d, $J = 4.8$ Hz, 1H); 7.56 (d, $J = 4.8$ Hz, 1H); 7.32 (d, $J = 9.6$ Hz, 1H); 6.88 (d, $J = 9.6$ Hz, 1H); 6.46 (d, $J = 9.2$ Hz, 1H); 3.03 (t, $J = 7.2$ Hz,

2H); 2.80 (t, $J = 7.2$ Hz, 2H). ^{13}C NMR (500MHz, $\text{DMSO-}d_6$): δ (ppm): 172.11, 165.76, 160.82, 154.94, 142.20, 134.77, 131.94, 128.43, 124.48, 119.08, 118.73, 116.19, 115.26, 37.50 and 28.38; FT-IR (KBr pellet): 3063, 2598, 1732, 1624 ($>\text{C}=\text{O}_{\text{COO}^-}$), 1597, 1568, 1452, 1389, 1279, 1254, 1225, 1159, 1101, 997, 814, 748, 627, 592 and 461 cm^{-1} .

2.6 Single-crystal X-ray diffraction

X-ray quality single crystal of His-anthracene was obtained by a slow evaporation of a DMSO solution of the salt at room temperature. Single-crystal X-ray data were collected with $\text{MoK}\alpha$ radiation ($\lambda = 0.7107\text{ \AA}$) using a SMART APEX-II diffractometer equipped with a CCD area detector (table 1). Data collection, data reduction, and structure solution and refinement were carried out using the SMART APEX-II software package. The structure was solved by direct methods and refined in a routine manner. The non-hydrogen atoms were treated anisotropically (figure 1). Whenever possible, the hydrogen atoms were geometrically fixed. Hydrogen bonding parameters are given in table 2.

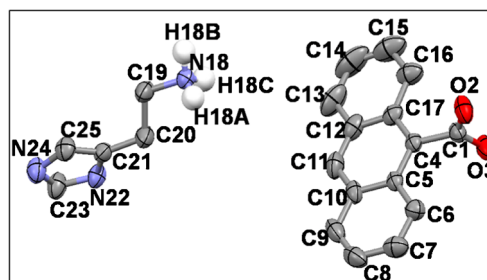


Figure 1. ORTEP plot (50% probability) of His-anthracene.

3. Results and Discussion

As discussed in the introduction section, RIR is the key to induce AIE or AEE. Anchoring luminigenic moiety on polymer chain is a well-known strategy to incorporate RIR. We thought that a similar effect can also be induced via supramolecular way, i.e., by making supramolecular polymer via hydrogen bonding. Organic salt formation is one such easy way towards supramolecular polymer synthesis. By judicious choice of acid and amine, it is possible to generate 1D, 2D, 3D and 0D hydrogen bonded network in organic salt

Table 1. Crystal data.

Crystal parameters	His-anthracene
CCDC No.	1001247
Empirical formula	$\text{C}_{20}\text{H}_{19}\text{N}_3\text{O}_2$
Formula weight	333.38
Crystal size/mm	0.55x 0.28 x 0.05
Crystal system	Orthorhombic
Space group	$P2(1)2(1)2(1)$
$a/\text{\AA}$	10.2623(5)
$b/\text{\AA}$	11.3590(6)
$c/\text{\AA}$	14.7950(8)
$\alpha/^\circ$	90
$\beta/^\circ$	90
$\gamma/^\circ$	90
Volume/ \AA^3	1724.65(16)
Z	4
$D_{\text{calc}}/\text{gcm}^{-3}$	1.284
F(000)	704
$\mu\text{MoK}\alpha/\text{mm}^{-1}$	0.085
Temperature/K	100(2)
R_{int}	0.0246
Range of h, k, l	-14/14, -14/15, -21/21
$\theta_{\text{min}}/\theta_{\text{max}}/^\circ$	2.26/31.23
Reflections collected/unique/ observed [$I > 2\sigma(I)$]	26724/ 3088/ 2488
Data/restraints/ parameters	3088/0/231
Goodness of fit on F^2	1.076
Final R indices	$R_1 = 0.0440$
[$I > 2\sigma(I)$]	$wR_2 = 0.1314$
R indices (all data)	$R_1 = 0.0587$
	$wR_2 = 0.1478$

Table 2. Hydrogen bonding parameters of His-anthracene.

D-H...A	D-H (Å)	H...A (Å)	D...A (Å)	D-H...A (°)	Symmetry operation for A
N(18)—H(18A)...N(24)	0.89	1.94	2.828(2)	176.1	-x+1, y+1/2, -z+1/2
N(18)—H(18B)...O(3)	0.89	1.90	2.776(2)	168.7	x, y-1, z
N(18)—H(18C)...O(2)	0.89	2.10	2.857(2)	142.4	x+1/2, -y+3/2, -z
N(18)—H(18C)...O(3)	0.89	2.40	3.179(2)	146.9	x+1/2, -y+3/2, -z
N(22)—H(22)...O(2)	0.88(3)	1.83(3)	2.705(2)	168(3)	x+1, y-1, z

and we have been contributed significantly towards the design of supramolecular gelators by exploiting various hydrogen bonded network via salt formation.¹⁸ In the present study, we decided to exploit salt formation strategy to induce AEE in the resulting of three well-known fluorophoric compounds with histamine. All these acids studied herein are monocarboxylic acid and thus, reacting them with a primary amine would expectedly give rise to 1D hydrogen bonded network namely primary ammonium mono-carboxylate synthon which can be considered as a supramolecular polymeric chain with the fluorophoric moieties anchored along the chain. Although such arrangement would predictively impart RIR, it might still provide some room for intramolecular rotation. In order to ensure maximum RIR, we chose to react acids with histamine which is a primary amine having additional hydrogen bonding site (imidazole moiety). The N acceptor and N-H donor of the imidazole moiety are expected to participate in hydrogen bonding resulting in 3D hydrogen bonding network thereby restricting the ⁻COO-fluorophoric moiety completely. Thus, the salts were prepared by mixing the acid and the amine in 1:1 molar ratio in MeOH at rt. FT-IR data clearly indicated salt formation (COO⁻ stretching band at 1624-1645 cm⁻¹). Figure 2 displays

the fluorescence spectra of the dilute solutions (10⁻⁴ M in MeOH) of the salts.

The salt His-pyrene showed the most intense photoluminescence (PL) ($\lambda_{\text{ex}} = 340$ nm; $\lambda_{\text{em}} = 398$ nm). The PL of His-anthracene showed a sharp structured spectra ($\lambda_{\text{ex}} = 380$ nm; $\lambda_{\text{em}} = 391, 407, 431, 457$ nm) relatively less intense than that of His-pyrene. His-coumarin, on the other hand, displayed almost negligible fluorescent spectrum and appeared flat when plotted against the fluorescence spectra of the other two salts. Interestingly, all the three salts displayed enhanced emission in their bulk solid state (figure 3). In the solid state, His-anthracene displayed the most intense structured PL spectrum ($\lambda_{\text{ex}} = 380$ nm; $\lambda_{\text{em}} = 420, 443, 469$ nm) whereas the PL spectra of both His-coumarin and His-pyrene were broad and significantly less intense than that of His-anthracene. The solution state PL spectra of the corresponding salts were almost negligible compared to the spectra in the solid state (figure 3). Thus, it was clear that all the salts displayed AEE in their solid state.

To study how exactly the hydrogen bonding network imposed RIR in the solid state, we tried to crystallize all the salts. Our best efforts resulted in the crystallization of X-ray quality single crystals of the salt His-anthracene. SXRD study revealed that the crystals belonged to the non-centrosymmetric space group P2₁2₁2₁ (table 2). The asymmetric unit was comprised of one ion-pair. The anthracene moiety of the mono-anion was found to be nearly planar and oriented almost orthogonally with the COO⁻ moiety displaying a dihedral angle of 89.0° involving the anthracene moiety and COO⁻. In the crystal structure, the carboxylate moiety was bound to three cationic species via various N-H...O interactions [$\text{N}\cdots\text{O} = 2.705(2)\text{--}3.179(2)$ Å; $\angle\text{N-H}\cdots\text{O} = 142.4\text{--}168.7^\circ$]; the carboxylic acid O atoms accepted two ammonium H atoms of two cationic species and one imidazole NH atom of another cation. The imidazole N acceptor was hydrogen bonded with the ammonium N via N-H...N interactions [$\text{N}\cdots\text{N} = 2.828(2)$ Å; $\angle\text{N-H}\cdots\text{N} = 176.1^\circ$]. Such hydrogen bonding interactions led to the formation of 2D hydrogen bonded sheet structures which were further packed in parallel fashion sustained

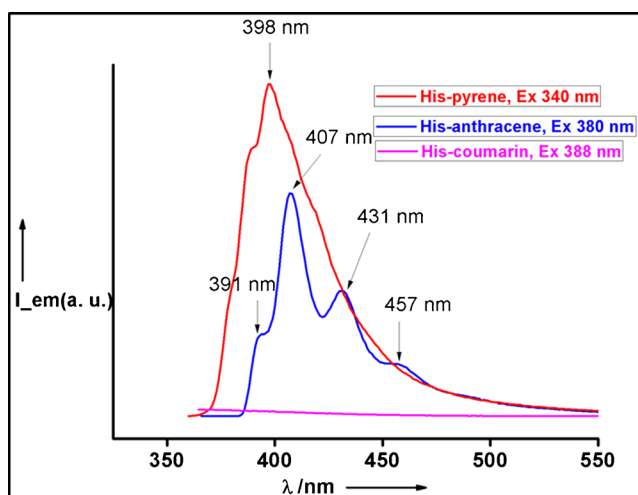


Figure 2. PL spectra of 10⁻⁴ M methanolic solution of His-pyrene (red), His-anthracene (blue) and His-coumarin (magenta).

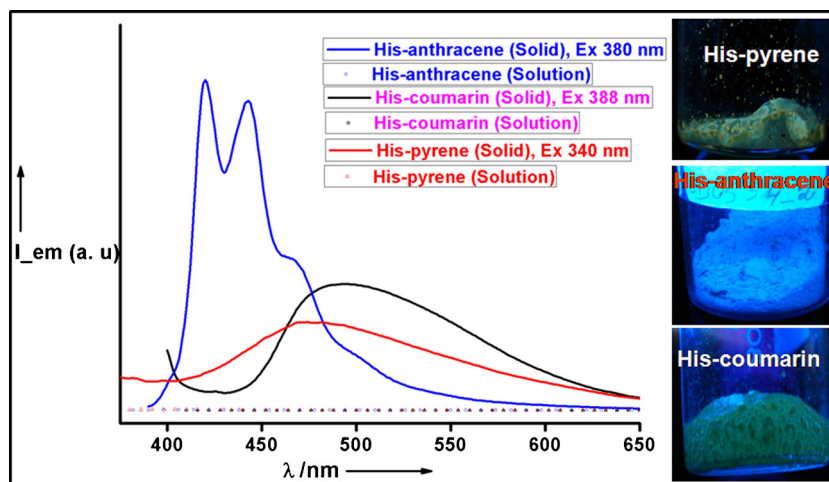


Figure 3. PL spectra of bulk solid of His-anthracene (blue), His-coumarin (magenta) and His-pyrene (red) in comparison with that of the corresponding solutions (10^{-4} M in MeOH) (Flat spectra).

by N-H \cdots O and N-H \cdots N interactions involving the COO $^{-}$ -ammonium and imidazole-ammonium moieties resulting in an overall 3D Hydrogen bonded network (figure 4). The distance between two adjacent parallel anthracene moieties is 10.26 Å. The distance between two centroids of adjacent non-parallel anthracene moieties is 7.8 Å. There is no $\pi\cdots\pi$ interactions. There are C-H $\cdots\pi$ interactions (3.84 Å) present between methylene group adjacent to ammonium moiety of histamine and the anthracene moiety; imidazole C-H and anthracene moiety (3.88 Å) and C-H of terminal ring of

one anthracene moiety (3.68 Å) with the terminal ring of another adjacent anthracene moiety.

The luminogenic anthracene moiety in the crystal structure of the salt His-anthracene was surrounded by three cationic species and one symmetry related anthracene carboxylate. Thus, there was no room for the anthracene moiety to undergo rotation around C-C bond of anthracene C and COO $^{-}$ C atom ensuring maximum RIR in this salt that was reflected in the solid state photoluminescence spectra of the salt. In the absence of the crystal structure of the other two salts, we cannot make definitive comment on the structural environment of the

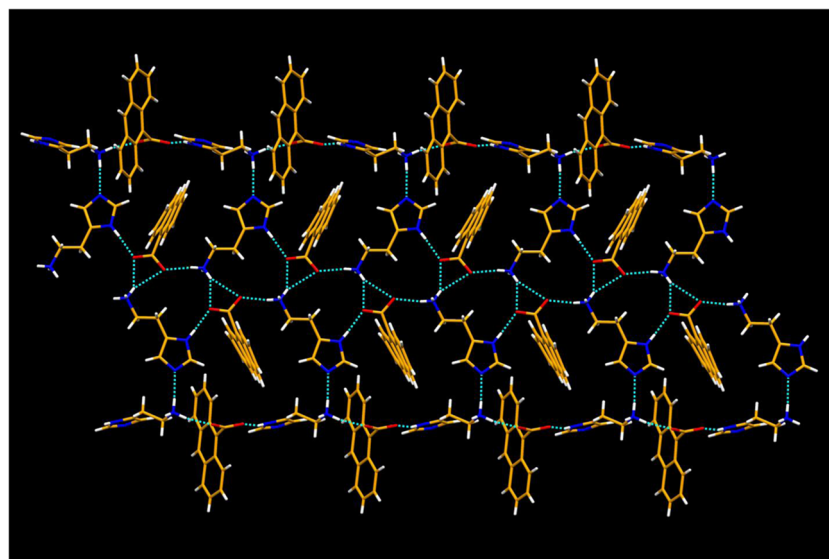


Figure 4. Crystal structure illustration for His-anthracene: View of 2D hydrogen bonded sheet sustained by N-H \cdots O and N-H \cdots N interactions.

fluorophoric moiety in the crystal structures. The fact that the other two salts also displayed significant AEE indicated the existence of RIR in these salts as well.

4. Conclusion

Among these salts, in the solution state, His-anthracene was the most PL active followed by His-pyrene whereas His-coumarin displayed almost negligible PL. Interestingly, in the crystalline (aggregated) state, His-coumarin was significantly PL active – in fact, the second most intense amongst the three salts wherein His-anthracene being the strongest. Single crystal structure of His-anthracene revealed the presence of the expected 3D hydrogen bonding network within which the luminogenic moiety namely anthracene was surrounded by the cationic as well as symmetry related anionic species thereby imposing significant RIR that resulted in emission enhancement in the solid state as compared to that of in the solution state. Thus we have demonstrated that salt formation – the easiest reaction to carry out – can serve as a simple strategy to get an easy access to materials capable of displaying AEE or AIE. Owing to the easy preparative method (salt formation), commercial availability and virtually infinite combination of the acids and amines, and strong and directional charge assisted hydrogen bonding useful in real-life fabrication of materials, the methodology demonstrated herein offers an attractive and expectedly commercially viable approach towards the design of photonic materials.

Supplementary Information

CCDC No. 1001247 contains the supplementary crystallographic data for this paper. These data can be obtained free of charge from The Cambridge Crystallographic Data Centre via www.ccdc.cam.ac.uk/data_request/cif.

Acknowledgement

UKD thanks CSIR and IACS for fellowships. PD thanks IACS for infrastructure and financial support. Professor Amitava Patra, IACS is also thanked for solid state PL measurements in his laboratory.

References

1. Lakowicz J R 1999 In *Principles of Fluorescence Spectroscopy* (New York: Kluwer Academic / Plenum Publishers) p 6
2. Thomas III S W, Joly G D and Swager T M 2007 *Chem. Rev.* **107** 1339
3. Barks B 1970 In *Photophysics of Aromatic Molecules* (London: Wiley)
4. Thompson R B 2006 In *Fluorescence Sensors and Biosensors* (Boca Raton: CRC)
5. Tang C W and Vanslyke S A 1987 *Appl. Phys. Lett.* **51** 913
6. Geddes C D and Lakowicz J R 2005 In *Advanced Concepts in Fluorescence Sensing* (Norwell: Springer)
7. Jares-Erijman E A and Jovin T M 2003 *Nat. Biotechnol.* **21** 1387
8. Saigusa H and Lim E C 1995 *J. Phys. Chem.* **99** 15738
9. Luo J, Xie Z, Lam J W Y, Cheng L, Chen H, Qiu C, Kwok H S, Zhan X, Liu Y, Zhu D and Tang B Z 2001 *Chem. Commun.* 1740
10. Tang B Z, Zhan X, Yu G, Lee P P S, Liu Y and Zhu D 2001 *J. Mater. Chem.* **11** 2974
11. Wu Y T, Kuo M Y, Chang Y T, Shin C C, Wu T C, Tai C C, Cheng T H and Liu W S 2008 *Angew. Chem. Int. Ed.* **47** 9891
12. Chen J, Law C C W, Lam J W Y, Dong Y, Lo S M F, Williams I D, Zhu D and Tang B Z 2003 *Chem. Mater.* **15** 1535
13. Grimme S 2008 *Angew. Chem. Int. Ed.* **47** 3430
14. Shimizu M, Takeda Y, Higashi M and Hiyama T 2009 *Angew. Chem. Int. Ed.* **48** 3653
15. An B K, Kwon S K, Jung S D and Park S Y 2002 *J. Am. Chem. Soc.* **124** 14410
16. Liu J, Lam J W Y and Tang B Z 2009 *Chem. Rev.* **109** 5799
17. Qin A, Jim C K W, Tang Y, Lam J W Y, Liu J, Mahtab F, Gao P and Tang B Z 2008 *J. Phys. Chem. B* **112** 9281
18. Dastidar P 2008 *Chem. Soc. Rev.* **37** 2699